First-principles insights into tin-based two-dimensional halide perovskites for photovoltaics

Zhenyu Wang,[†,‡,¶] Alex M. Ganose,[‡,¶,§] Chunming Niu,[†] and David O. Scanlon[*,‡,¶,§]

†*Xi'an Jiaotong University, Center of Nanomaterials for Renewable Energy, State Key Lab of Electrical Insulation and Power Equipment, School of Electrical Engineering, 99 Yanxiang Road, Xi'an 710054, China*

‡*University College London, Kathleen Lonsdale Materials Chemistry, Department of Chemistry, 20 Gordon Street, London WC1H 0AJ, UK*

¶*Thomas Young Centre, University College London, Gower Street, London WC1E 6BT, UK*

§*Diamond Light Source Ltd., Diamond House, Harwell Science and Innovation Campus, Didcot, Oxfordshire OX11 0DE, UK*

E-mail: d.scanlon@ucl.ac.uk

Supporting Information

Details of the spectroscopic limited maximum efficiency (SLME)

In the spectroscopic limited maximum efficiency (SLME) metric,[1] a photovoltaic cell is treated as an ideal diode illuminated under the incident photon flux I_{sun}, and the total

current can be calculated as follows,

$$J = J_{sc} - J_0(1 - e^{\frac{eV}{k_B T}}), \tag{1}$$

where V is the potential over the absorber thin film, k_B Boltzmann's constant, T the temperature, respectively.

J_{sc} is the the short-circuit current density given by,

$$J_{sc} = e\int_0^\infty a(E)I_{sun}(E)dE = e\int_0^\infty (1 - exp(-2\alpha(E)L))I_{sun}(E)dE, \tag{2}$$

where α and L are the absorption coefficient and thickness of the thin film, respectively.

J_0 is reverse saturation current given by,

$$J_0 = f_r^{-1}J_0^r = ef_r^{-1}\int_0^\infty a(E)I_{bb}(E,T)dE = ef_r^{-1}\int_0^\infty (1 - exp(-2\alpha(E)L))I_{bb}(E,T)dE, \tag{3}$$

$$f_r = e^{-\Delta/(k_B T)}, \tag{4}$$

where I_{bb}, f_r^{-1} and Δ are the black-body radiation flux, fraction of the radiative recombination current and difference between the lowest direct allowed transition and the fundamental band gaps, respectively.

The maximum energy conversion efficiency, $SLME$, is given by,

$$SLME = \frac{[JV]_{max}}{P_{in}}, \tag{5}$$

where $[JV]_{max}$ and P_{in} are the maximum electrical output power density and the total incident solar power density, respectively.

Table S1: Lattice parameters of $(BA)_2(MA)_{n-1}Sn_nI_{3n+1}$ unit cells using PBE-D3

Compounds	a (Å)	b(Å)	c(Å)	α (°)	β (°)	γ (°)
$(BA)_2SnI_4{}^{rt}$	8.497	8.724	28.034	90.0	90.0	90.0
$(BA)_2SnI_4{}^{lt}$	8.410	8.911	26.074	90.0	90.0	90.0
$(BA)_2(MA)Sn_2I_7$	20.230	20.230	8.479	95.0	95.0	25.5
$(BA)_2(MA)_2Sn_3I_{10}$	8.551	9.085	25.307	90.5	97.7	90.9

Table S2: Lattice parameters of $(BA)_2(MA)_{n-1}Sn_nI_{3n+1}$ conventional cells using PBE-D3 and PBEsol in comparison with experiment

Compounds	Functional	a (Å)	b(Å)	c(Å)	α (°)	β (°)	γ (°)
$(BA)_2SnI_4{}^{rt}$	PBE-D3	8.497	8.724	28.034	90.0	90.0	90.0
	PBEsol	8.519	8.691	28.411	90.0	90.0	90.0
	Ref. 2	8.591	8.814	27.644	90.0	90.0	90.0
$(BA)_2SnI_4{}^{lt}$	PBE-D3	8.410	8.911	26.074	90.0	90.0	90.0
	PBEsol	8.334	8.839	26.807	90.0	90.0	90.0
	Ref. 2	8.408	8.932	26.023	90.0	90.0	90.0
$(BA)_2(MA)Sn_2I_7$	PBE-D3	39.458	8.946	8.479	90.0	95.1	90.0
	PBEsol	40.026	8.968	8.394	90.0	92.8	90.0
	Ref. 3	39.497	8.858	8.776	90.0	90.0	90.0
$(BA)_2(MA)_2Sn_3I_{10}$	PBE-D3	8.551	50.184	9.085	89.4	90.9	92.0
	PBEsol	8.461	51.440	9.031	89.6	90.9	91.5
	Ref. 4	8.795	51.921	8.858	90.0	90.0	90.0

Table S3: Average in-plane and out-of-plane Born effective charges (Z^*) over Sn and I atoms. Superscripts $\parallel$ and $\perp$ indicate properties parallel (in-plane) and perpendicular (out-of-plane) to the 2D perovskite sheets, respectively

Compounds	Atom	$Z^*_{\parallel}$	$Z^*_{\perp}$
$(BA)_2SnI_4{}^{rt}$	Sn	4.916	2.601
	I	-2.035	-1.000
$(BA)_2(MA)Sn_2I_7$	Sn	4.992	2.984
	I	-2.000	-1.226
$(BA)_2(MA)_2Sn_3I_{10}$	Sn	5.011	3.467
	I	-2.197	-1.386

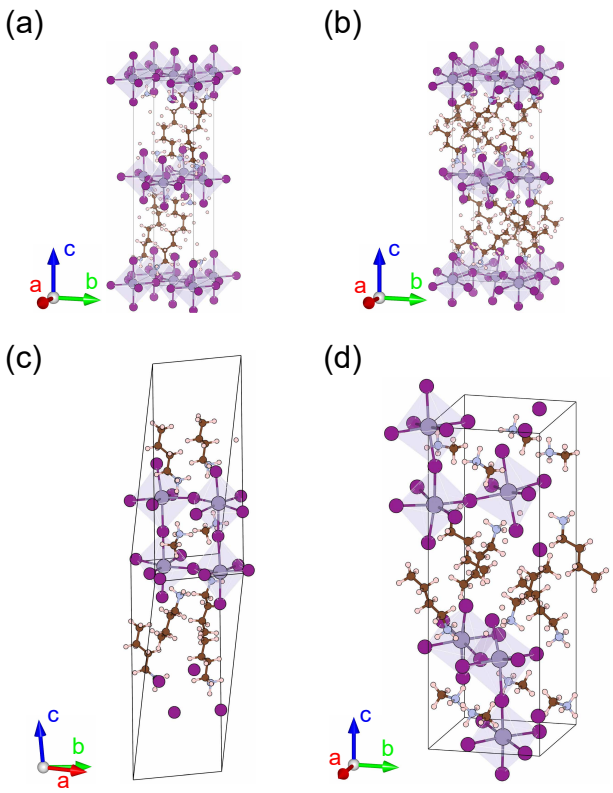

Figure S1: Crystal structures of the layered tin hybrid perovskites unit cells: (a) $(BA)_2SnI_4^{rt}$, (b) $(BA)_2SnI_4^{lt}$, (c) $(BA)_2(MA)Sn_2I_7$, and (d) $(BA)_2(MA)_2Sn_3I_{10}$

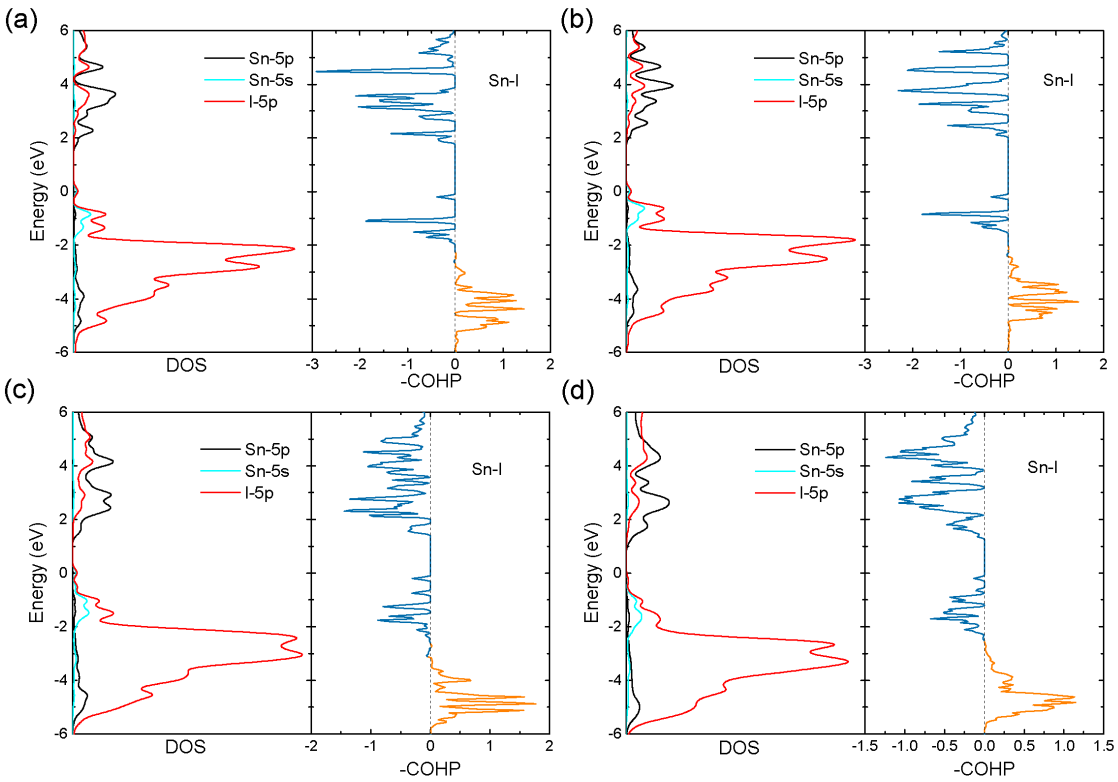

Figure S2: Projected density of states (PDOS) and "inverted" crystal orbital Hamilton populations (-COHP) of Sn–I bonds for the layered tin hybrid perovskites: (a) $(BA)_2SnI_4^{rt}$, (b) $(BA)_2SnI_4^{lt}$, (c) $(BA)_2(MA)Sn_2I_7$, and (d) $(BA)_2(MA)_2Sn_3I_{10}$, where the energy is with respect to the Fermi level. Since the "inverted" COHP values are plotted, the positive regions (orange line) represent the bonding interactions , while the negative regions (blue line) denote antibonding interactions.

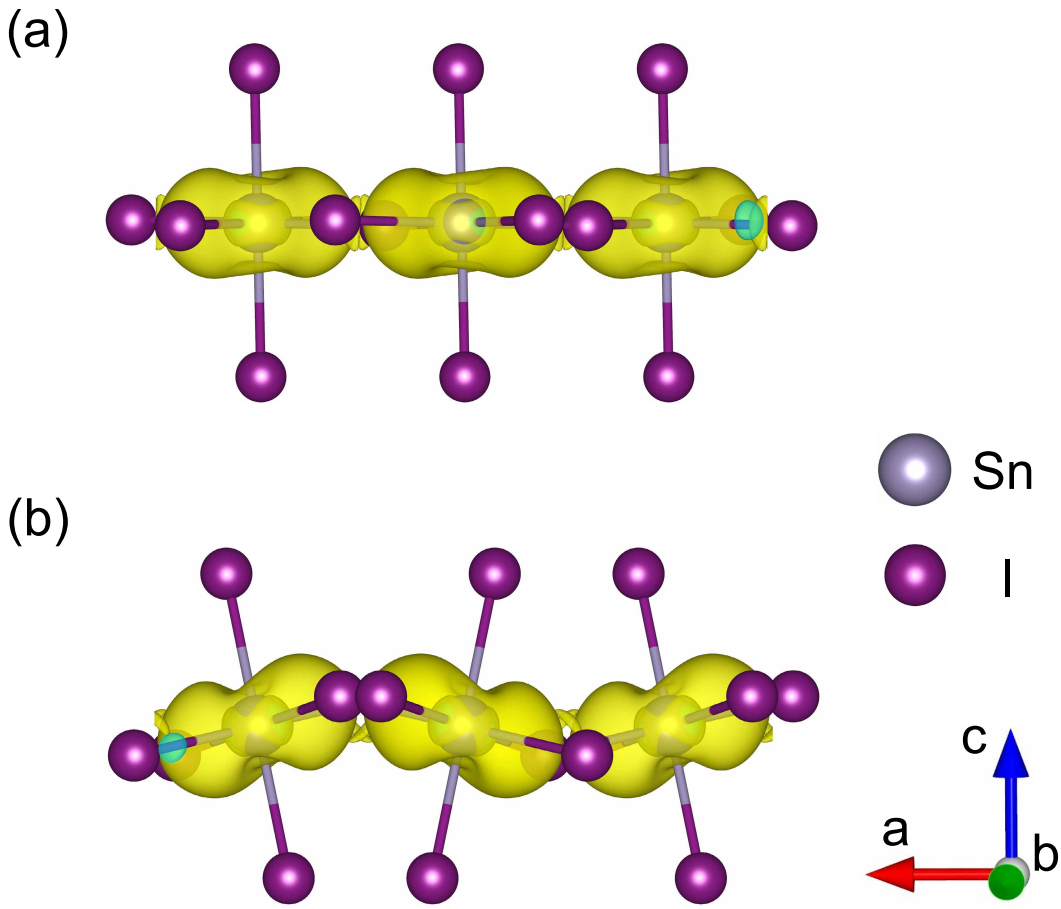

Figure S3: Charge density isosurfaces of the conduction band minimum (CBM) of the SnI_6^{4-} octahedra in (a) $(BA)_2SnI_4{}^{rt}$ and (b) $(BA)_2SnI_4{}^{lt}$.

References

(1) Yu, L.; Zunger, A. Identification of potential photovoltaic absorbers based on first-principles spectroscopic screening of materials. *Phys. Rev. Lett.* **2012**, *108*, 068701.

(2) Takahashi, Y.; Obara, R.; Nakagawa, K.; Nakano, M.; Tokita, J.-y.; Inabe, T. Tunable Charge Transport in Soluble Organic–Inorganic Hybrid Semiconductors. *Chem. Mater.* **2007**, *19*, 6312–6316.

(3) Stoumpos, C. C.; Mao, L.; Malliakas, C. D.; Kanatzidis, M. G. Structure-Band Gap

Relationships in Hexagonal Polytypes and Low-Dimensional Structures of Hybrid Tin Iodide Perovskites. *Inorg. Chem.* **2017**, *56*, 56–73.

(4) Mitzi, D. B.; Feild, C.; Harrison, W.; Guloy, A. Conducting tin halides with a layered organic-based perovskite structure. *Nature* **1994**, *369*, 467–469.